# Computational consequences of experimentally derived spike-time and weight dependent plasticity rules

Dominic Standage, Sajiya Jalil and Thomas Trappenberg

Faculty of Computer Science
Dalhousie University, Halifax, Canada

**Biological Cybernetics (2007) 96:615-623**

**Abstract**

We present two weight- and spike-time dependent synaptic plasticity rules consistent with the physiological data of Bi and Poo (1998). One rule assumes synaptic saturation, while the other is scale free. We extend previous analyses of the asymptotic consequences of weight-dependent STDP to the case of strongly correlated pre- and post-synaptic spiking, more closely resembling associative learning. We further provide a general formula for the contribution of any number of spikes to synaptic drift. Asymptotic weights are shown to principally depend on the correlation and rate of pre- and post-synaptic activity, decreasing with increasing rate under correlated activity, and increasing with rate under uncorrelated activity. Spike train statistics reveal a quantitative effect only in the pre-asymptotic regime, and we provide a new interpretation of the relation between BCM and STDP data.

# 1 Introduction

Change in synaptic efficacy is believed to underlie learning and memory and has long been established in the forms of long term potentiation (LTP) (Bliss & Lomo, 1973) and long term depression (LTD) (Lynch, Dunwiddie, & Gribkoff, 1977). Experimental and theoretical work on plasticity has addressed the dependence of plasticity on pre-synaptic firing rates (Bienenstock, Cooper, & Munro, 1982; Dudek & Bear, 1992; Kirkwood, Rioult, & Bear, 1996), the timing (Levy & Steward, 1983; Markram, Lbke, Frotscher, & Sakmann, 1997; qiang Bi & ming Poo, 1998) and interaction (Sjostrom, Turrigiano, & Nelson, 2001; Bi, 2002; Froemke & Dan, 2002; Izhikevich & Desai, 2003; Wang, Gerkin, Nauen, & Bi, 2005; Froemke, Tsay, Raad, Long, & Dan, 2006; Shah, Yeung, Cooper, Cai, & Shouval, 2006) of pre- and post-synaptic spikes, and initial synaptic strength or *weight* (qiang Bi & ming Poo, 1998; Debanne, Gahwiler, & Thompson, 1999; Montgomery, Pavlidis, & Madison, 2001; Wang et al., 2005). Theoretical studies have further investigated the relationship between rate based and spike-time dependent plasticity (STDP) frameworks (Izhikevich & Desai, 2003; Burkitt, Meffin, & Grayden, 2004) and the conditions under which STDP rules transduce correlations among pre-synaptic spike trains into correlations between pre- and post-synaptic activity (Kempter, Gerstner, & van Hemmen, 1999; Kistler & van Hemmen, 2000; Kuhn, Aertsen, & Rotter, 2003; Gutig, Aharonov, Rotter, & Sompolinsky, 2003) as required by Hebb's postulate (Hebb, 1949).

Here, we focus on weight-dependent STDP rules. In Section 2, we derive parameters for two weight-dependent STDP rules from experimental data. We calculate asymptotic weights resulting from these rules in Section 3. Where earlier studies of the asymptotic consequences of STDP rules consider uncorrelated or weakly correlated pre- and post-synaptic spike trains (Kempter et al., 1999; Kistler & van Hemmen, 2000; Song, Miller, & Abbott, 2000; van Rossum, Bi, & Turrigiano, 2000; Rubin, Lee, & Sompolinsky, 2001; Gutig et al., 2003; Burkitt et al., 2004), we extend these analyses to the case of strongly correlated spikes, where pre-synaptic activity 'repeatedly and persistently takes part in firing' the post-synaptic cell, as proposed by Hebb. Our analysis shows that the means of equilibrium weight distributions are principally determined by the correlation and rate of pre- and post-synaptic spiking, where weights decrease with increasing rate in the correlated case. In Section 4, we show that our qualitative results do not depend on our choice of spike train statistics or correlation model. Furthermore, we derive

a general formula for the contribution of any number of individual spikes to synaptic drift, proving that our results do not depend on a specific implementation of spike interactions, in contrast to the interpretation of Izhikevich and Desai (2003). We end Section 4 by showing a novel instance of rate-based BCM curves (Bienenstock et al., 1982) under STDP. These curves emerge when temporal constraints prevent weights from reaching asymptotic values at lower spike rates.

# 2 Weight dependence of STPD

Weight-dependent plasticity has been shown by several groups (qiang Bi & ming Poo, 1998; Debanne et al., 1999; Montgomery et al., 2001; Wang et al., 2005), but only Bi and Poo (1998) have done so under the STDP pairing protocol. Not only did they use the same protocol in their weight- and spike-time-dependent experiments, but they controlled spike timing in their weight-dependent experiment, allowing us to relate these two data sets. We therefor derive our weight-dependent plasticity rules from their data.

For simplicity, our analysis of weight- and spike-time-dependent plasticity assumes these two factors are independent. A learning rule of this form may be written as

$$\Delta w_{\{p,d\}} = k f_{\{p,d\}}(w) e^{-c_{\{p,d\}}\Delta t}, \tag{1}$$

where $\Delta w_{\{p,d\}}$ is the change in weight for potentiation (index $p$) or depression (index $d$), $\Delta t = t_{post} - t_{pre}$ is the difference between the times of post-synaptic ($t_{post}$) and pre-synaptic ($t_{pre}$) firing, and $c$ parameterizes the timescale of the plasticity window. The experimental data are commonly shown in relative terms (%) whereas our formulations express absolute changes in synaptic strength.

We consider two forms of the weight dependent factor $f$. Bi and Poo (1998) hypothesized a log-linear rule by drawing a line through these data in the semi-logarithmic plot. This hypothesis yields

$$f_{\{p,d\}}(w) = (a_{\{p,d\}} - b_{\{p,d\}} \log w) w \; \theta(w), \tag{2}$$

where $\theta(w)$ is the Heaviside function, keeping weights positive, and the parameters $a$ and $b$ differ for potentiation and depression. A maximum weight implicit in this rule agrees with evidence for saturable synapses (Petersen,

Malenka, Nicoll, & Hopfield, 1998; O'Connor, Wittenberg, & Wang, 2005b). We contrast the above rule with a power rule of the form

$$f_{\{p,d\}}(w) = a_{\{p,d\}} w^{b_{\{p,d\}}}. \tag{3}$$

A power law more closely approximates the data plotted on a log scale, and, unlike the log rule, imposes no maximum weight. While synapses must surely have intrinsic limits, we include this rule for comparison with the limited case. We hereafter refer to Equation 1 with weight-dependence determined by Equations 2 and 3 as the Log and Power rules respectively.

The constants in Equations 2 and 3 were determined by first fitting the weight-dependent STDP data shown in Figure 1B. The fitted curves for the Log rule are shown as solid lines alongside the potentiation data (circles) and depression data (stars) of Bi and Poo (1998). The equivalent curves for the Power rule are shown as dashed lines. The fits to the depression data are nearly indistinguishable. The fits to the potentiation data agree similarly with the data, but the intrinsic limit in the Log rule generates a marked difference for large weight values.

## 2.1 Detailed fitting procedure

Bi and Poo (1998) controlled spike timing in their weight-dependent experiment by limiting their pre-before-post (LTP) time interval to $5 < \Delta t < 15$ms and limiting their post-before-pre (LTD) interval to $3 < \Delta t < 30$ms. For the weight-dependent fit, we replaced these intervals with their midpoint values ($\Delta t_p = 10, \Delta t_d = 17.5$). We then fit their spike-time dependent data (Figure 1B) to determine the remaining parameter $c$ in Equation 1, capturing the time course of spike-time dependence for each of potentiation and depression. Because of the wide range of initial synaptic strengths in Bi and Poo's spike-time dependent experiment ($30 < w < 500$pA) we assumed that for a given $\Delta t$, the largest relative changes in weight represent synapses with the smallest initial values. Thus, consistent with their initial weights, we assign an initial weight $w = 30$pA to the data showing the largest STDP values, and only include these data in our time-dependent fit determining $c$. The resulting parameter values are $a_{\{p,d\}} = \{208, -54\}$, $b_{\{p,d\}} = \{26.4, 3.5\}$, $c_{\{p,d\}} = \{0.054, 0.042\}$ for the Log rule and $a_{\{p,d\}} = \{431, -59\}$, $b_{\{p,d\}} = \{0.4, 0.1\}$, $c_{\{p,d\}} = \{0.039, 0.043\}$ for the Power rule. We further assume that each of the 60 pre-before-post pairings in the experiment contributed equally

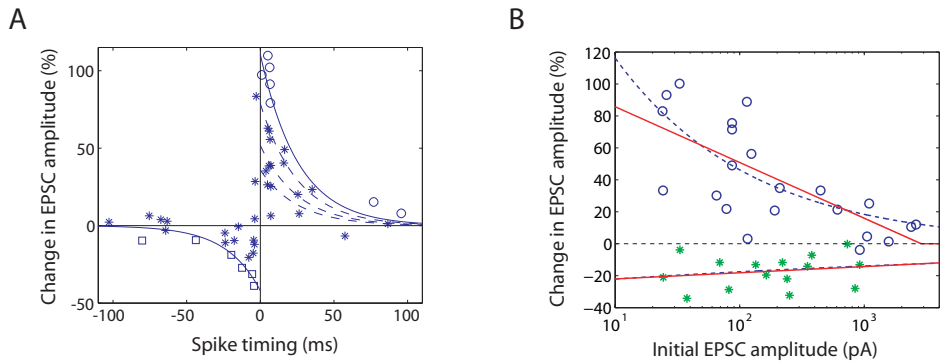


Figure 1: (A) Fit of the Power rule to Bi and Poo's (1998) spike-time dependent data for estimates of different initial weights $w$. Circles and squares represent $w = 30$ for potentiation and depression respectively. Solid curves show fits to these data. Dashed curves for the potentiation data show fits for $w = \{70, 200, 500\}$pA top to bottom. The Log rule leads to similar fits. (B) Log and power fits to Bi and Poo's weight-dependent STDP data. A log fit imposes a maximum synaptic weight where the upper solid line meets the x-axis. A power fit (dashed curve) imposes no such maximum. These two fits are nearly indistinguishable for the LTD data.

to the overall synaptic change. This assumption is common in computational studies (van Rossum et al., 2000). A deviation from this linear assumption results in an altered learning rate that does not effect the means of equilibrium weight distributions. As the above parameters are deduced by fitting the percentage data, we include a factor of 100 in the learning rate to yield a fractional scale. The learning rate used in our analyses and simulations is therefore $k = 1/6000$ unless otherwise stated.

Fitted curves for the Power rule are shown as solid lines in Figure 1A for our estimates of the data representing initial weights of 30pA (open symbols). The large scatter in the figure is commonly interpreted as noise, but we interpret it according to the weight-dependence shown in Figure 1B. For potentiation, we include dashed lines representing initial weights set to 70, 200 and 500 pA respectively (top to bottom). The fit of the Log rule leads to qualitatively similar plots.

# 3 Equilibrium weights for uncorrelated and time-locked pre- and post-synaptic Poisson spike trains

While the above plasticity rules are deterministic, they yield a stochastic drift of weights with stochastic spike trains. If this drift is driven by a novel correlation between pre- and post-synaptic spiking, weights will undergo considerable change from an initial random state. When weights have been driven for long periods by pre- and post-synaptic spiking with a given statistical profile, they begin to fluctuate around a mean value where the average potentiation equals the (negative) average depression. In this section, we calculate the means of these equilibrium weight distributions for the Log and Power rules. The drift of weights can be calculated with Fokker-Planck mean field theory (Kempter et al., 1999; Kistler & van Hemmen, 2000; van Rossum et al., 2000; Rubin et al., 2001; Burkitt et al., 2004), but we are concerned with the means of equilibrium distributions and adopt the simplified methodology of Izhikevich and Desai (2003). We refer to these asymptotic values as equilibrium weights $w^*$.

First, we present our basic analysis for the cases of uncorrelated and time-locked pre- and post-synaptic spike trains (see Figure 2A) where these spike trains are Poisson distributed (Bair, Koch, Newsome, & Britten, 1994) (exponential inter-spike intervals) and where only *nearest neighbour* spikes contribute to plasticity. Under nearest neighbour STDP, each pre-synaptic spike triggers LTP with the next post-synaptic spike and triggers LTD with the previous post-synaptic spike, as described by Izhikevich and Desai (2003). In Section 4, we show that our qualitative results do not change for partially correlated spike trains or for other spike train distributions or spike interactions.

## 3.1 Equilibrium weights for uncorrelated Poisson spiking

The average synaptic increase (LTP) for each pre-synaptic spike is given by

$$\langle \Delta w_p \rangle = \int_0^\infty p_p(\Delta t) \Delta w_p d\Delta t, \tag{4}$$

where $p_p(\Delta t)$ is the probability density of a post-synaptic spike following a

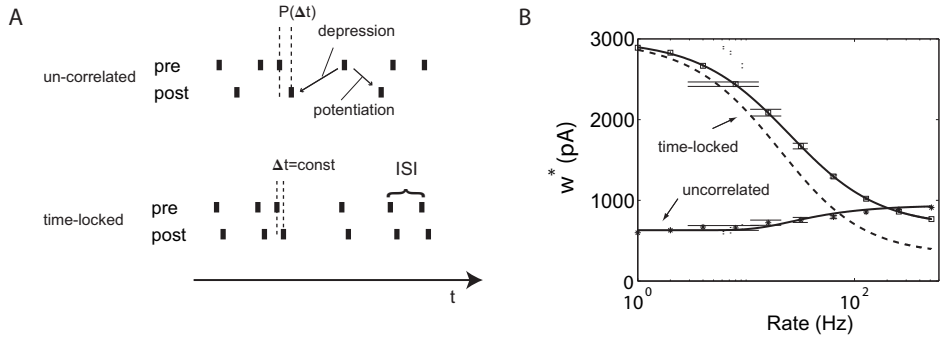


Figure 2: (A) Illustration of uncorrelated and time-locked spike trains. (B) Equilibrium weights as a function of spike rate under the Log rule for analytic (curves) and numeric (symbols with error bars) calculations. For time-locked spiking, the solid and dashed curves correspond to $\Delta t = 4$ and $\Delta t = 10$ms respectively. In numeric simulations, weights were averaged over 5000 trials following an equilibrating 5000 trials.

pre-synaptic spike with time lag $\Delta t$. Similarly, the average depression for each pre-synaptic event is given by

$$\langle \Delta w_d \rangle = \int_0^\infty p_d(\Delta t) \Delta w_d d\Delta t, \tag{5}$$

where $p_d(\Delta t)$ is the probability density of a post-synaptic spike preceding a pre-synaptic spike with time lag $\Delta t$. Thus, independent pre- and post-synaptic Poisson spike trains have an average depression and potentiation of

$$\begin{aligned} \langle \Delta w_{\{p,d\}} \rangle &= f_{\{p,d\}}(w) \int_0^\infty r e^{-(c_{\{p,d\}}+r)\Delta t} d\Delta t & (6) \\ &= f_{\{p,d\}}(w) \frac{r}{c_{\{p,d\}} + r}, & (7) \end{aligned}$$

where $r$ is the rate of the spike trains. We only consider the case where $r_{\rm pre} = r_{\rm post} = r$.

An equilibrium weight $w^*$ is reached when the average potentiation equals the (negative) average depression. For the Log rule this value is given by

$$w^* = \exp \frac{a_p(c_d + r) + a_d(c_p + r)}{b_p(c_d + r) + b_d(c_p + r)} \tag{8}$$

and for the Power rule by

$$w^* = (-\frac{a_p}{a_d}\frac{c_d + r}{c_p + r})^{\frac{1}{b_d - b_p}}. \quad (9)$$

Equilibrium weights for independent pre- and post-synaptic Poisson spike trains are shown as a function of rate in Figure 2B for the Log rule. Symbols represent the results of simulations where weights were averaged over 5000 spike pairings following 5000 equilibrating pairings.

## 3.2 Equilibrium weights for time-locked Poisson spiking

The above analysis of uncorrelated pre- and post-synaptic spikes is relevant if events represented by pre-synaptic firing are *not* associated with a post-synaptic response. In contrast, associative learning is achieved if a neuron becomes responsive to (correlated with) a pre-synaptic spike pattern. Studies have shown that STDP rules capture correlations among input spikes driving a model neuron (Kistler & van Hemmen, 2000; Song et al., 2000), as synapses mediating correlated pre-synaptic activity learn to provide the strongest, fastest (Song et al., 2000) and most precisely timed (Kistler & van Hemmen, 2000) inputs to the post-synaptic cell. Alternatively, plasticity may 'piggyback' other sources of activity driving pre- and post-synaptic neurons. In this section, we assume associations have been formed by one or both of these mechanisms, labelled self-organisation and associativity respectively under the terminology of Hasselmo (Hasselmo, 1995). We investigate the ongoing effect of these associations on the asymptotic strength of weights for rules grounded in Bi and Poo's data (qiang Bi & ming Poo, 1998).

For analytic simplicity and to illustrate the limiting case for informative spike timing, we consider the case where a post-synaptic spike is triggered with a short but fixed delay $\Delta t$ following a pre-synaptic spike. We do not suggest that a single pre-synaptic spike should drive a post-synaptic neuron in this way. Rather, our pre-synaptic spikes represent the activity of one of many inputs from pre-synaptic neurons participating in an established association. We later relax this condition by varying the probability of a time-locked post-synaptic spike in Section 4.1.

Time-locked pre- and post-synaptic spikes result in an ongoing potentiation of weights given by

$$\langle \Delta w_p \rangle = f_p(w) e^{-c_p \Delta t} \tag{10}$$

for each pre-synaptic event. However, every pre-synaptic event can also trigger depression in conjunction with a previous (uncorrelated) post-synaptic spike (Equation 6). An equilibrium weight $w^*$ for correlated pre- and post-synaptic spikes under the Log rule is therefore given by

$$w^* = \exp \frac{a_p e^{-c_p \Delta t}(c_d + r) + a_d r}{b_p e^{-c_p \Delta t}(c_d + r) + b_d r} \tag{11}$$

and for the Power rule by

$$w^* = (-\frac{a_p}{a_d} \frac{1}{r} e^{-c_p \Delta t} \ (r + c_d))^{\frac{1}{b_d - b_p}}. \tag{12}$$

The rate-dependence of equilibrium weights for time-locked pre- and post-synaptic Poisson activity under the Log rule is shown in Figure 2B, where the solid and dashed lines represent analytic solutions for $\Delta t = 4$ms and $\Delta t = 10$ms respectively. Symbols represent corresponding numeric simulations. The figure shows that equilibrium weights decrease with increasing spike rates in the strongly correlated Poisson case, but quantitatively, these values exceed biologically realistic values.

# 4 Equilibrium weights for alternative conditions

In the previous section, we determined equilibrium weights for the Log and Power rules under the specific conditions of Poisson-distributed pre- and post-synaptic spike trains, uncorrelated and time-locked pre- and post-synaptic spikes, and nearest neighbour spike interactions. Here, we show in Section 4.1 that partially correlated pre- and post-synaptic spike trains interpolate between the extreme cases of uncorrelated and time-locked pre- and post-synaptic spikes. We show in Section 4.2 that our results do not qualitatively depend on Poisson-distributed spike trains. In Section 4.3, we show that our results do not depend on nearest neighbour spike interactions, in contrast to the claims of Izhikevich and Desai (2003). Finally, in Section 4.4, we demonstrate learning under a finite number of spike pairings, and discuss how BCM-like curves (Bienenstock et al., 1982) are generated by the Log and Power rules.

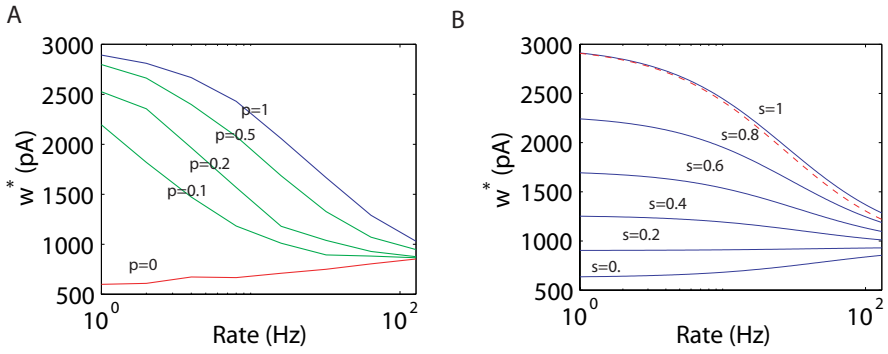


Figure 3: (A) Correlation model with varying probability $p$ of a time locked post-synaptic spike. Weights were averaged over 5000 trials following 5000 equilibrating trials. (B) Correlation model with varying exponential distribution for different correlation parameters $s$ where $\Delta_t = r/(1-s)$. The dashed line shows the time looked case discussed in section 3.2 with $\Delta t = 1$ms.

## 4.1 Equilibrium weights for partially correlated pre- and post-synaptic Poisson spiking

The cases of uncorrelated and time-locked pre- and post-synaptic spike trains define the extreme cases of possible spike train relations. Here we extend this analysis to some more realistic cases with partially correlated pre- and post-synaptic activity. We discuss two examples of correlation models, providing a biological interpretation of each. In both models, we again consider Poisson pre-synaptic spiking.

**Correlation model 1:** Post-synaptic spikes are generated with a probability given by constant $p$ with a fixed time delay $\Delta t = 4$ms. In the $(1-p)$ cases where there is no time-locked post-synaptic spike the time delay is distributed exponentially. This methodology approximates the biological case where pre-synaptic input generates a post-synaptic spike with a finite probability, but otherwise the post-synaptic neuron emits Poisson background activity. Figure 3A shows mean weights over 10,000 pairings following 10,000 equilibrating pairings under the Log rule for $p = \{0, 0.2, 0.4, 0.6, 0.8, 1\}$. Low values of $p$ lead to rate-dependent curves qualitatively similar to the perfectly time-locked case ($p = 1$) where lower means reflect the lower likelihood of correlated pre- and post-synaptic spikes.

**Correlation model 2:** We consider the case where correlations between pre- and post-synaptic spikes are expressed by an altered probability of a post-synaptic spike within a time $\Delta t$ of a pre-synaptic event. Specifically, we consider an exponential distribution of delay times $\Delta t$, where the decay parameter is modulated for different correlations between pre- and postsynaptic spikes. The alteration of the probability density of $\Delta t$ is accomplished by parameter $s$ in Equation 13. The mean delay $\Delta t$ is set to be $(1-s)\lambda$, where $\lambda = 1/r$ is the inverse of the spike rate. For $s = 0$, this parameter yields the uncorrelated case discussed above. When $s$ tends to 1, we expect a post-synaptic spike with a very short average time delay. The average potentiation (and similarly for depression) and the corresponding equilibrium weights are given by

$$\Delta w_p = (a_p - b_p \log w) w \int_0^\infty \frac{r}{1-s} e^{-(\frac{r}{1-s}+c_p)\Delta t} d\Delta t \tag{13}$$

$$\Leftrightarrow w^* = \exp \frac{a_p(1/((1-s)c_p+1) + a_d(1/(c_d+r))}{b_p(1/((1-s)c_p+1) + b_d(1/(c_d+r))}. \tag{14}$$

Analytic equilibrium weights for this correlation model are plotted in Figure 3B for different values of $s$, where $s = 0$ is equivalent to the uncorrelated case in Figure 2B and $s = 1$ is close to the time looked case with $\Delta t = 1$ms, shown with a dashed line in the figure. Both correlation models show that partial pre- and post-synaptic correlations interpolate the extreme cases discussed in Section 3.

## 4.2 Equilibrium weights for spike trains with non-Poisson statistics

We have thus far shown results for Poisson spike trains in our analysis, but similar derivations can be made for other spike distributions. While the specific values of equilibrium weights for a given rate depend on the distribution model, their qualitative dependence on rates and the correlation between pre- and post-synaptic spiking does not change. Examples from simulations for several ISI distributions are shown in Figure 4. Figure 4A shows the cases of uncorrelated and time-locked pre- and post-synaptic spikes under the Log rule. Figure 4B shows the time-locked case under the Power rule. The dependence of equilibrium weights on rate is similar for these distribu-

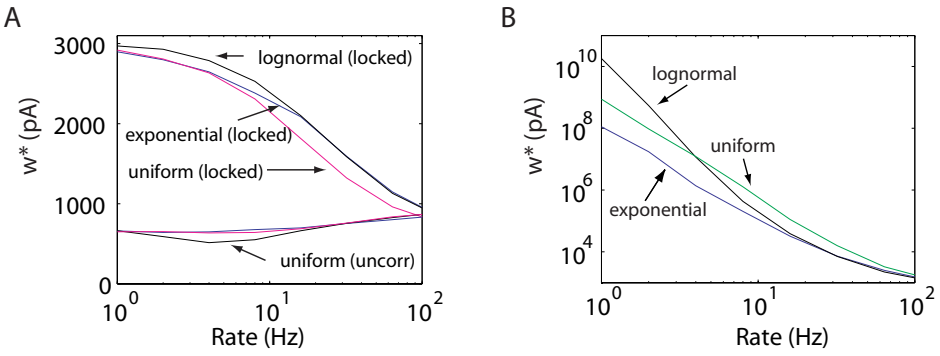


Figure 4: Equilibrium weights as a function of rate for pre- and post-synaptic spike trains with different ISI distributions. (A) Time-locked (top) and uncorrelated (bottom) spiking with the Log rule. (B) Time-locked spiking with the Power rule.

tions, but could possibly differ for very different distributions such as those corresponding to bursting behaviour.

## 4.3 Equilibrium weights beyond nearest neighbour interactions

In the nearest neighbour case, we only consider the first post-synaptic spike following a pre-synaptic spike for potentiation and the first pre-synaptic spike following a post-synaptic spike for depression. While the first spike makes the greatest contribution to plasticity due to the decaying exponential term in STDP rules, it is possible that the sum of subsequent spikes has a pronounced effect on synaptic strength, as argued by Izhikevich and Desai (2003).

For Poisson spike trains, we use the following method to analytically calculate the average contribution to potentiation of the $n$-th spike following a specific pre-synaptic spike (the method is the same for depression, where pre-synaptic spikes follow a specific post-synaptic spike). The first post-synaptic spike is expected to occur on average at $\Delta t_1 = 1/r$ for uncorrelated pre- and post-synaptic activity, and at $\Delta t_1 = \text{const}$ in the time locked case, and is weighted by $e^{-c_p \Delta t_1}$. The second spike, which we expect on average at $\Delta t_2 = \Delta t_1 + 1/r$, contributes less to potentiation because $e^{-c_p \Delta t_1} < e^{-c_p \Delta t_2}$. To calculate the average potentiation, we determine the density function of the $n$-th spike by convolving the density functions of all random variables in

the sum. This convolution can be done analytically for Poisson spike trains by independently summing exponentially distributed random variables with equal mean $\lambda$. The resulting random variable is gamma distributed with mean $\lambda = 1/r$ and parameter $n$,

$$p(\Delta t_n) = \frac{(\Delta t/\lambda)^{n-1} e^{-\Delta t/\lambda}}{\lambda \Gamma(n)} \tag{15}$$

where $n$ is the number of spikes considered. Thus, the average potentiation for uncorrelated pre- and post-synaptic spike trains is given by

$$\langle \Delta w_p \rangle = k f_{\{p,d\}}(w) \sum_{n=1}^{N} \int_0^\infty r^n (\Delta t)^{n-1} \frac{e^{-(r+c_p)\Delta t}}{\Gamma(n)} d\Delta t \tag{16}$$

and similarly for depression. Using the definition of the Gamma function,

$$\Gamma(x) = \int_0^\infty e^{-t} t^{x-1} dt, \tag{17}$$

we can evaluate this integral as

$$\langle \Delta w_p \rangle = k f_{\{p,d\}}(w) \sum_{n=1}^{N} \left( \frac{r}{r + c_p} \right)^n, \tag{18}$$

generalizing equation (7) to multiple spike contributions. Thus, equilibrium weights for the uncorrelated case are given for the Log rule by

$$w^* = \exp \frac{a_p \sum_{n=1}^{N} (c_d + r)^n + a_d \sum_{n=1}^{N} (c_p + r)^n}{b_p \sum_{n=1}^{N} (c_d + r)^n + b_d \sum_{n=1}^{N} (c_p + r)^n}, \tag{19}$$

which reduces to equation (8) for $n = 1$. Furthermore, since

$$\sum_{n=1}^{\infty} x^n = \frac{1}{x - 1} \quad \text{for } x < 1, \tag{20}$$

where $x = r/(r + c_{\{p,d\}})$, the all-to-all case for uncorrelated spike trains is independent of $r$,

$$w^*(n = \infty) = \exp \frac{a_p c_d + a_d c_p}{b_p c_d + b_d c_p}, \tag{21}$$

in agreement with (Kempter et al., 1999). This value is also equivalent to the $r = 0$ limit for $n = 1$ (eq. 8).

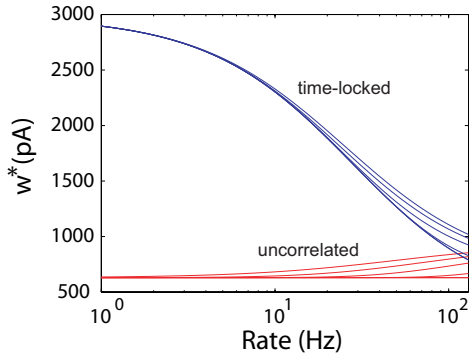


Figure 5: Equilibrium weights under *nearest-n* interactions for time-locked and uncorrelated Poisson spike trains. In each case, curves correspond to values of $n = \{1, 2, 4, 10, 50, 100\}$ (top to bottom). Curves between $n = 50$ and $n = 100$ become indistinguishable and approximate the infinite (asymptotic) case.

A similar evaluation for the time-locked case yields

$$w^* = \exp \frac{a_p \Delta P + a_d \Delta D}{b_p \Delta P + b_d \Delta D} \tag{22}$$

with

$$\Delta P = e^{-c_p \Delta t}(1 + \sum_{n=2}^{N} \frac{r^{n-1}(n-2)!}{(c_p + r)^{n-1}\Gamma(n-1)}) \tag{23}$$

and

$$\Delta D = \sum_{n=1}^{N} \frac{r^n (n-1)!}{(c_p + r)^n \Gamma(n)}. \tag{24}$$

Equilibrium values for interaction models with different $n$ (*nearest-n* interactions) are shown in Figure 5 for the time-locked and independent Poisson cases. These curves correspond to values of $n = \{1, 2, 4, 10, 50, 100\}$ (from top to bottom) although results between $n = 50$ and $n = 100$ become indistinguishable. As expected, an increasing number of neighbouring spikes will only influence equilibrium values at high rates due to the exponential decay of the STDP time window. Furthermore, increasing the number of neighbours $n$ quickly converges to an asymptotic value. We reached machine precision around $n = 150$.

## 4.4 Convergence to equilibrium: BCM-like curves in the pre-asymptotic regime

The analysis above concerns the asymptotic regime, where equilibrium weights correspond to the infinite limit of pairings, and simulations approximate this limit with many thousands of pairings. Experiments in vitro are temporally constrained in that a plasticity-inducing stimulus is applied for a short time, after which synaptic responses are measured and compared to pre-stimulus measurements. While the duration of plasticity-inducing stimuli typically varies across protocols and the nature of experiments, the number of repetitions is typically on the order of 10 to 100 for STDP (qiang Bi & ming Poo, 1998; Froemke & Dan, 2002) and pairing protocols (Petersen et al., 1998; O'Connor, Wittenberg, & Wang, 2005a) and 100 to 1000 repetitions for rate-based protocols (Dudek & Bear, 1992; Kirkwood et al., 1996). We now consider the effects of the Log and Power rules under similar conditions.

Figure 6A shows mean percentage weight changes following $n = 100$ spike pairings where weights were initialised in the middle range of possible values (700pA) and means were calculated over 100 trials. In this simulation, we use Poisson spike trains under the Log rule with nearest neighbour spike interactions. Results for uncorrelated pre- and post-synaptic spikes correspond to the case studied by Izhikevich and Desai (2003). While we can generate BCM-like curves in this limited case of finite pairings and uncorrelated spiking, the effect is small and not found in the time-locked case. Results for time-locked spikes resemble those in the asymptotic regime (eg. Figure 2B) though here, percentage weight change is reduced by several orders of magnitude.

We can, however, show BCM-like curves with different spike train statistics. Figure 6B shows that BCM-like curves resembling those measured by Dudek and Bear (1992) and Kirkwood and Rioult (1996) are produced with time-locked, periodic pre- and post-synaptic spiking ($\Delta t = \frac{1000}{2r}$ms). Results are shown for the Log rule. The solid line represents weight changes after 1000 pairings for a synapse initialised to 700pA. Performing the same experiment with 10,000 spike pairings results in the dashed line. The dotted line corresponds to weight changes for an infinite number of pairings (equilibrium weights). As shown in the figure, the depression valley becomes deeper and shifts to the left with an increased number of pairings, while changes in the potentiation portion of the curve are much smaller. Our investigation shows that BCM-like curves may be produced by STDP rules in the pre-asymptotic

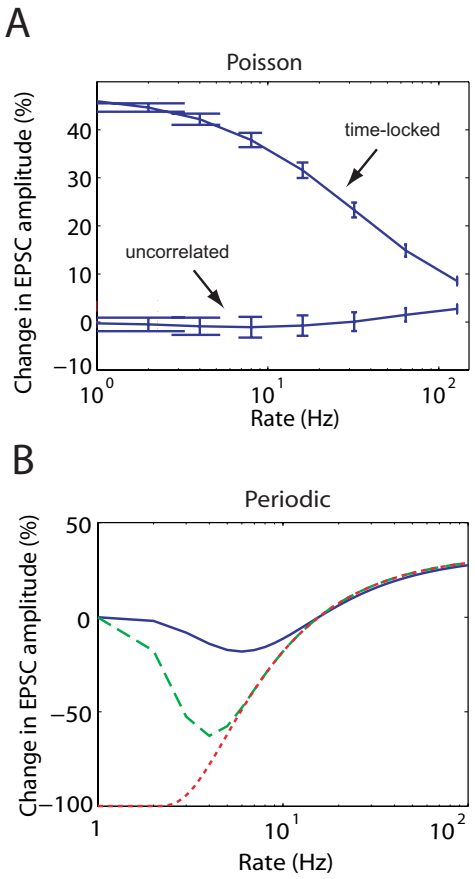


Figure 6: Mean percentage weight change under the Log rule for limited numbers of spike pairings. Weights were initialised to mid-range values (700pA) and means were calculated over 100 trials. (A) Results for time-locked and uncorrelated Poisson spike trains for 100 pairings at rate $r$ with nearest neighbour spike interactions. (B) Results for periodic, time-locked pre- and post-synaptic spike trains where pre- and post-synaptic spikes are 180 degrees out of phase. The solid line shows changes after 1000 pairings for a synapse initialised to 700pA. The same experiment with 10,000 spike pairings results in the dashed line. The dotted curve shows analytic equilibrium, corresponding to an infinite number of pairings.

regime, but these curves depend on the precise form of pre- and post-synaptic firing. Further experiments are required to investigate this and other possible explanations for BCM-like curves, as experiments investigating BCM (Dudek & Bear, 1992; Kirkwood et al., 1996) have not controlled post-synaptic firing, crucial to the BCM hypothesis.

# 5 Discussion and Conclusions

Weight-dependent STDP rules are commonly used in modelling studies. We have presented two such rules with parameters fit to physiological data (qiang Bi & ming Poo, 1998) and studied their consequences in both the asymptotic and pre-asymptotic regimes. Our analysis includes the case where synapses are driven by noisy spike trains with little or no correlation between pre- and post-synaptic spikes, as done in previous studies, and also the case of highly correlated pre- and post-synaptic spike trains more closely resembling the case of associative learning. We found that 'runaway' synapses (Abbott & Nelson, 2000) are still a problem for these rules, at least under parameters suggested by weight-dependent STDP data (qiang Bi & ming Poo, 1998).

In the pre-asymptotic regime, we show that BCM-like curves (Bienenstock et al., 1982) can be generated by weight-dependent STDP rules when low-rate activity prevents weights from reaching equilibrium values in finite time. While this effect is parameter dependent, it provides a novel instance of these curves and highlights the need for rate-based plasticity experiments that control post-synaptic spiking.

In the asymptotic regime, we find that for all spike train statistics considered, equilibrium weights for correlated spike trains decrease with increasing spike rate, a novel form of synaptic scaling. We prove this relationship for an arbitrary number of contributing spikes in the Poisson case, providing a general formula for the drift of potentiation and depression in the steady state. We further demonstrate this relationship for partially correlated Poisson spiking, showing that partial correlations interpolate between the extreme cases of time-locked and independent pre- and post-synaptic activity.

Equilibrium weights for uncorrelated spike trains increase with rate for a finite number of contributing spikes. This increase approaches 0 in the infinite limit of spike contributions, showing rate independence in this specific case, consistent with the analysis of Kempter and Gerstner (1999). Correlated and independent equilibrium weights converge at around 100Hz. This effect

suggests that low to intermediate rates provide a better regime for associative learning than high rates, or, stated differently, high rates may prevent weights from distinguishing between correlated and uncorrelated activity.

Under a rule imposing no maximum weight (the Power rule) synapses do not reach infinite values because depression balances potentiation, but the resulting equilibrium values under both rules (with and without maxima) are too large to be useful in a biologically realistic regime. This problem has an additional, unwanted consequence. Weight-dependent STDP rules implicitly assume that a synapse can span the entire range of values in Bi and Poo's weight-dependent STDP data (qiang Bi & ming Poo, 1998), suggesting changes in synaptic efficacy of around $10,000\%$. No synapse in their experiments, however, changed in strength by more than around 100%. Many more pairings than the 60 of their protocol would be required to traverse this range, assuming their synapses could in fact be further strengthened. Alternatively, it is possible that the large variation in their initial weights (Figure 1B) reflects varying populations of synapses. Neurons in culture often make multiple post-synaptic contacts (Debanne, Gahwiler, & Thompson, 1996) and this possibility must be carefully addressed in future experiments on weight-dependent STDP.

# Acknowledgment

We thank Alan Fine and Stefan Kruger for helpful discussions. This work was supported in part by the NSERC grant RGPIN 249885-03.

# References

Abbott, L. F., & Nelson, S. B. (2000). Synaptic plasticity: taming the beast. *Nature Neuroscience*, *3*, 1178–1183.

Bair, W., Koch, C., Newsome, W., & Britten, K. (1994). Power spectrum analysis of bursting cells in area mt in the behaving monkey. *Journal of Neuroscience*, *14*(5), 2870–2892.

Bi, G.-Q. (2002). Spatiotemporal specificity of synaptic plasticity: cellular rules and mechanisms. *Biological Cybernetics*, *87*, 319–332.

Bienenstock, E. L., Cooper, L. N., & Munro, P. W. (1982). Theory for the development of neuron selectivity: orientation specificity and binocular interaction in visual cortex. *Journal of Neuroscience*, *2*(1), 32–48.

Bliss, T. V. P., & Lomo, T. J. (1973). Long-lasting potentiation of synaptic transmission in the dentate area of the anaesthetized rabbit following stimulation of the perforant path. *Journal of Physiology*, *232*, 331–356.

Burkitt, A., Meffin, H., & Grayden, D. B. (2004). Spike-timing-dependent plasticity: The relationship to rate-based learning for models with weight dynamics determined by a stable fixed point. *Neural Computation*, *16*, 885–940.

Debanne, D., Gahwiler, B. H., & Thompson, S. M. (1996). Cooperative interactions in the induction of long-term potentiation and depression of synaptic excitation between hippocampal ca3-ca1 cell pairs in vitro. *Proceedings of the National Academy of Sciences of the United States of America*, *93*, 11225–11230.

Debanne, D., Gahwiler, B. H., & Thompson, S. M. (1999). Heterogeneity of synaptic plasticity at unitary ca3-ca1 and ca3-ca3 connections in rat hippocampal slice cultures. *Journal of Neuroscience*, *19*(24), 10664–10671.

Dudek, S. M., & Bear, M. F. (1992). Homosynaptic long-term depression in area ca1 of hippocampus and effects of n-methyl-d-aspartate receptor blockade. *Proceedings of the National Academy of Sciences of the United States of America*, *89*, 4363–4367.

Froemke, R. C., & Dan, Y. (2002). Spike-timing-dependent synaptic modification induced by natural spike trains. *Nature*, *416*(6879), 433–438.

Froemke, R. C., Tsay, I. A., Raad, M., Long, J. D., & Dan, Y. (2006). Contribution of individual spikes in burst-induced long-term synaptic modification. *Journal of Neurophysiology*, *95*, 1620–1629.

Gutig, R., Aharonov, R., Rotter, S., & Sompolinsky, H. (2003, May). Learning input correlations through nonlinear temporally asymmetric hebbian plasticity. *Journal of Neuroscience*, *23*, 3697–3714.

Hasselmo, M. E. (1995). Neuromodulation and cortical function: modeling the physiological basis of behavior. *Behavioural Brain Research*, *67*, 1–27.

Hebb, D. O. (1949). *The organisation of behaviour*. John Wiley, New York.

Izhikevich, E. M., & Desai, N. S. (2003). Relating stdp to bcm. *Neural Computation*, *15*(7), 1511–1523.

Kempter, R., Gerstner, W., & van Hemmen, J. L. (1999). Hebbian learning

and spiking neurons. *Physical Review E*, *59*(4), 4498–4514.

Kirkwood, A., Rioult, M. G., & Bear, M. F. (1996). Experience-dependent modification of synaptic plasticity in visual cortex. *Nature*, *381*, 526–528.

Kistler, W. M., & van Hemmen, J. L. (2000). Modeling synaptic plasticity in conjunction with the timing of pre- and postsynaptic action potentials. *Neural Computation*, *12*, 385–405.

Kuhn, A., Aertsen, A., & Rotter, S. (2003). Higher-order statistics of input ensembles and the response of simple model neurons. *Neural Computation*, *15*, 67–101.

Levy, W. B., & Steward, O. (1983). Temporal contiguity requirements for long-term associative potentiation/depression in the hippocampus. *Neuroscience*, *8*, 791–797.

Lynch, G., Dunwiddie, T., & Gribkoff, V. (1977). Heterosynaptic depression: a postsynaptic correlate of long-term potentiation. *Nature*, *266*, 737–739.

Markram, H., Lbke, J., Frotscher, M., & Sakmann, B. (1997). Regulation of synaptic efficacy by coincidence of postsynaptic aps and epsps. *Science*, *275*(5297), 213–215.

Montgomery, J. M., Pavlidis, P., & Madison, D. V. (2001). Pair recordings reveal all-silent synaptic connections and the postsynaptic expression of long-term potentiation. *Neuron*, *29*, 691–701.

O'Connor, D. H., Wittenberg, G. M., & Wang, S. S.-H. (2005a). Dissection of bidirectional synaptic plasticity into saturable unidirectional processes. *Journal of Neurophysiology*, *94*, 1565–1573.

O'Connor, D. H., Wittenberg, G. M., & Wang, S. S.-H. (2005b). Graded bidirectional synaptic plasticity is composed of switch-like unitary events. *Proceedings of the National Academy of Sciences of the United States of America*, *102*(27), 9679–9684.

Petersen, C. C., Malenka, R. C., Nicoll, R. A., & Hopfield, J. J. (1998). All-or-none potentiation at ca3-ca1 synapses. *Proceedings of the National Academy of Sciences of the United States of America*, *95*, 4732–4737.

qiang Bi, G., & ming Poo, M. (1998). Synaptic modifications in cultured hippocampal neurons: Dependence on spike timing, synaptic strength, and postsynaptic cell type. *Journal of Neuroscience*, *18*, 10464–10472.

Rubin, J., Lee, D. D., & Sompolinsky, H. (2001). Equilibrium properties of temporally asymmetric hebbian plasticity. *Physical Review Letters*, *86*, 364.

Shah, N. T., Yeung, L. C., Cooper, L. N., Cai, Y., & Shouval, H. Z. (2006). A biophysical basis for the inter-spike interaction of spike-timing-dependent plasticity. *Biological Cybernetics*, *95*, 113–121.

Sjostrom, P. J., Turrigiano, G. G., & Nelson, S. B. (2001). Rate, timing, and cooperativity jointly determine cortical synaptic plasticity. *Neuron*, *32*, 1149–1164.

Song, S., Miller, K. D., & Abbott, L. F. (2000). Competitive hebbian learning through spike-timing-dependent synaptic plasticity. *Nature Neuroscience*, *3*(9), 919–926.

van Rossum, M. C. W., Bi, G. Q., & Turrigiano, G. G. (2000). Stable hebbian learning from spike timing-dependent plasticity. *Journal of Neuroscience*, *20*(23), 8812–8821.

Wang, H.-X., Gerkin, R. C., Nauen, D. W., & Bi, G.-Q. (2005). Coactivation and timing-dependent integration of synaptic potentiation and depression. *Nature Neuroscience*, *8*(2), 187–193.